J Clust Sci (2013) 24:1127–1137
DOI 10.1007/s10876-013-0603-2

ORIGINAL PAPER

Planar D_{2h} $B_{26}H_8$, D_{2h} $B_{26}H_8^{2+}$, and C_{2h} $B_{26}H_6$: Building Blocks of Stable Boron Sheets with Twin-Hexagonal Holes

Wen-Juan Tian · Hui Bai · Hai-Gang Lu · Yan-Bo Wu · Si-Dian Li

Received: 12 May 2013 / Published online: 27 June 2013

Abstract The most stable mono-layer boron sheets were predicted to have both the isolated hexagonal hole and the twin-hexagonal hole. Previous investigations indicate that planar $B_{18}H_n^q$ ($n = 3$–6, $q = n - 4$) are the building blocks of boron sheets with isolated hexagonal holes. Extensive DFT investigations performed in this work show that D_{2h} $B_{26}H_8$, D_{2h} $B_{26}H_8^{2+}$, and C_2 $B_{26}H_6$, may serve as the building blocks of boron sheets with twin-hexagonal holes. These bicyclic clusters possess planar or quasi-planar geometries at B3LYP/6-311+G(d,p) level, with 16, 14, and 14 delocalized π electrons, respectively. Detailed analyses indicate that they are overall aromatic in nature, with the formation of islands of both σ and π aromaticity. They are analogous to D_{2h} $C_{16}H_{14}$ and D_{2h} $C_{16}H_{14}^{2+}$ in π bonding patterns, respectively, but fundamentally different from the latter in σ-bonding. Remarkably, all of them appear to be energetically the lowest-lying isomers obtained, which are promising targets for future gas phase syntheses. These hydroboron clusters, together with $B_{18}H_n^q$ clusters, establish the molecular basis for modeling the short-range structures, nucleation, and growth processes of monolayer boron sheets. The results obtained in this work enrich the chemistry of boron

Electronic supplementary material The online version of this article (doi:10.1007/s10876-013-0603-2) contains supplementary material, which is available to authorized users.

W.-J. Tian · H. Bai · H.-G. Lu · Y.-B. Wu (✉) · S.-D. Li (✉)
Institute of Molecular Science, The Key Laboratory of Chemical Biology and Molecular Engineering of Education Ministry, Shanxi University, Taiyuan 030006, Shanxi, People's Republic of China
e-mail: wyb@sxu.edu.cn

S.-D. Li
e-mail: lisidian@sxu.edu.cn

S.-D. Li
Department of Chemistry, Institute of Material Science, Xinzhou Teachers' University, Xinzhou 034000, Shanxi, People's Republic of China

hydride clusters and expand the analogy relationship between hydroborons and hydrocarbons.

Keywords Boron hydrides · Twin-hexagonal holes · Double-chains · Aromaticity · Boron sheets

Introduction

Boron, the prototypical electro-deficient element, generally favors the three-dimensional cage structure in its elementary substances to guarantee the sufficient use of their valence electrons. Correspondingly, various crystalline boron and most of bottleable low-dimensional nanostructures of boron are known to be composed of icosahedral B_{12} units [1, 2]. In contrast, other geometries of boron have been long thought to be energetically too high to be synthesized. Nevertheless, experimental evidence for lamellar boron structures continues to accumulate. In addition to the realization of honeycomb (graphene-like) arrangement of boron in crystalline MgB_2 [3], experimental syntheses of single- and multiple-walled boron nanotubes [4, 5] strongly suggest the possibility of mono-layer boron sheets (MLBS). Theoretical instigations based on the first principle calculations also present possible realization of MLBS. Fully filled triangular sheet (planar close pack) is known to buckle due to the mismatch of the electronic structure to the geometrical structure [6–8]. Perfect planar MLBS can be stabilized by removing certain number of boron atoms from the triangular sheet to from stable hybrids of triangular and hexagonal motifs with the hexagonal hole density of $\eta_{m/n}$ ($\eta_{m/n}$ is defined as the ratio of the number of removed boron (m) to the total number of boron (n) of original triangular sheet in the unit cell). The previously reported α-sheet ($\eta_{1/9}$) [7] and α_1-sheet ($\eta_{1/8}$) [9] characterized with isolated hexagonal holes (IHHs) and $\eta_{2/14}$-sheet [10] and $\eta_{2/15}$-sheet [11] featured with twin-hexagonal holes (THHs) are the most stable unary boron sheets which lie close in energy (within 6 meV/atoms at PBE0 level) [10–12]. Using the ab initio global search method, our group recently revealed the binary nature of the most stable MLBSs including $\eta_{3/24}$ ($\eta_{1/9} \oplus \eta_{2/15}$), $\eta_{4/28}$ ($\eta_{1/14} \oplus \eta_{2/14}'$), $\eta_{4/33}$ ($2\eta_{1/9} \oplus \eta_{2/15}$), and other binary boron sheets with bigger unit cells. As specific combinations of the four unary boron sheets, these binary boron sheets turn out to be more stable than any of their component unary boron sheets [12]. Surprisingly and remarkably, $\eta_{4/28}$-sheet, the most stable boron sheet predicted so far which lies 6 meV more stable than the α-sheet at PBE0, is composed of solely THHs ($\eta_{4/28}$ is a combination of $\eta_{2/14}$ and its reversed $\eta_{2/14}'$) [12], further indicating the important and unique roles the THHs play in stabilizing MLBSs.

The analogy relationships between the small boron clusters and aromatic hydrocarbons are also intriguing in chemistry. The neutral and anionic bare boron clusters $B_n^{0/-q}$ with n up to 20 were found to be planar or quasi-planar [13–18], in which the analogy relationships between D_{7h} B_8^{2-}, D_{8h} B_9^-, C_{2h} B_{10}, and C_{3v} B_{12} (6 π-electrons) [13, 14] and D_{6h} C_6H_6 (benzene), that between C_1 B_{15}^- [14], D_{2h} B_{16}^{2-} [16] and C_{2v} B_{17}^- [18] (10 π-electrons) and D_{2h} $C_{10}H_8$ (naphthalene), and that between C_{2v} B_{19}^- [17] and C_{3v} B_{18}^- [18] (two sets of π-aromatic systems) and

D_{6h} $C_{24}H_{12}$ (coronene) have been well established. B_n^- monoanions were recently confirmed to be planar up to B_{23}^- [19]. Interestingly, partial hydrogenation of B_n clusters also leads to planarization in small boron-rich boron hydride clusters, as indicated in the cases of the elongated double-chain (DC) planar $B_nH_2^{0/-}$ ($n = 3$–12) [20], perfectly planar $B_6H_5^+$ [21], disk-like $B_{12}H_n^{0/-}$($n = 1$–4) [22, 23] and the elongated $B_{16}H_6^{0/-}$ [24] Remarkably, the DC planar $B_nD_2^-$ ($n = 7$–12) series were very recently confirmed by a joint photoelectron spectroscopy and theoretical investigation [25].

Our group proposed the first boron hydride clusters D_{3h} $B_{18}H_3^-$, D_{2h} $B_{18}H_4$, C_{2v} $B_{18}H_5^+$, and D_{6h} $B_{18}H_6^{2+}$ which are the smallest boron hydride clusters composed of a DC framework with a hexagonal hole at the center [26]. These monocyclic $B_{18}H_n^q$ clusters referred to as borannulenes appear to be analogous to the monocyclic planar $C_{10}H_{10}$ ([10] annulene) in π bonding and are predicted to be building blocks of MLBSs with IHHs. By fusing the borannulenes in specific manners, we construct in a recent report various polycyclic aromatic hydroboron clusters including $B_{30}H_8$, $B_{39}H_9^{2-}$, $B_{42}H_{10}$, $B_{48}H_{10}$, $B_{72}H_{12}$ which turn out to be analogous to polycyclic aromatic hydrocarbons in π bonding. Such polycyclic hydroboron clusters with a DC framework can be viewed as partially hydrogenated fragments of the snub-sheet [27].

In this work, we perform a systematical DFT investigation on the bicyclic planar D_{2h} $B_{26}H_8$ (**1a**), D_{2h} $B_{26}H_8^{2+}$ (**2a**), and C_{2h} $B_{26}H_6$ (**3a**) which are the smallest hydroboron clusters composed of a DC framework with a twin-hexagonal hole at the center. Such clusters are expected to serve as the building blocks of stable $\eta_{2/14}$, $\eta_{2/15}$, $\eta_{3/24}$, $\eta_{4/28}$, $\eta_{4/33}$ MLBSs with THHs. Detailed analyses indicate that they are overall aromatic in nature, with the formation of islands of both σ and π aromaticity. These hydroboron clusters appear to be energetically the lowest-lying isomers obtained and promising targets for future gas phase syntheses.

Computational Procedures

The first initial structure of bicyclic $B_{26}H_8$ was obtained as a partially hydrogenated fragment of the stable binary MLBSs with a twin-hexagonal hole at the center and a DC framework around it (see Fig. 1 and Fig. S1 in Electronic Supplementary Material). More planar, DC tubular, or cage-like structures were constructed arbitrarily according to chemical intuitions based on known small 2D and 3D B_n and B_nH_m clusters [13–25]. Such structures were then fully optimized at B3LYP [28, 29] level with 6-311+G(d,p) basis set, followed by harmonic frequencies analyses to verify the genuine minima and to evaluate the zero-point energy (ZPE) corrections. Initial structures for $B_{26}H_8^{2+}$ and $B_{26}H_6$ were obtained based on the corresponding low-lying $B_{26}H_8$. The five lowest-lying isomers thus obtained are shown in Fig. 1 and alternative isomers summarized in Fig. S2. Extensive structural searches using the Coalescence Kick (CK) algorithm [30, 31] produced various interesting low-lying isomers, but none has lower energies than the lowest-lying planar D_{2h} $B_{26}H_8$ (**1a**), D_{2h} $B_{26}H_8^{2+}$ (**2a**), and C_{2h} $B_{26}H_6$ (**3a**). The canonical molecular orbital (CMO) analyses at B3LYP/6-311+G(d,p) and the detailed

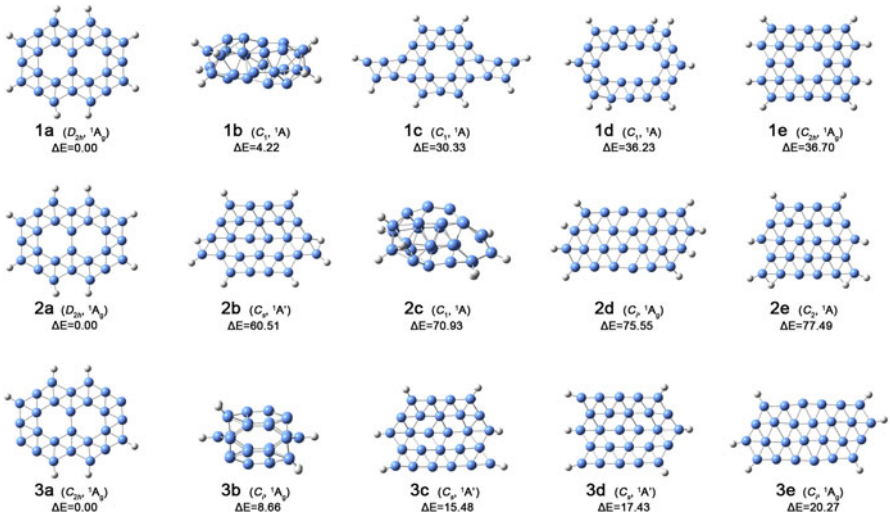

Fig. 1 B3LYP/6-311+G(d,p) geometries of the five lowest-lying isomers of $B_{26}H_8$, $B_{26}H_8^{2+}$ and $B_{26}H_6$ obtained, with relative energies (E, in kcal/mol) indicated

adaptive natural density partitioning (AdNDP) [32–34] analyses at B3LYP/6-31G were carried out to interpret their bonding patterns. The electron localization function (ELF) [35] at B3LYP/6-31G level (previous studies had suggested AdNDP and ELF analyses were basis set insensitive) and nucleus independent chemical shift (NICS) [36–38] analyses using gauge-independent atomic orbital (GIAO) [39] procedure at B3LYP/6-311+G(d,p) level were performed to access the overall and island aromaticity of the systems. The ionization potential (IPs) of the neutrals were calculated using the outer valence Green's function (OVGF) at OVGF/6-311+G(d,p). All the calculations in this work were performed using the Gaussian 09 package [40].

Results and Discussions

Structures and Stabilities

We start from a perfectly planar D_{2h} B_{26} which is a fragment of the $\eta_{2/14}$, $\eta_{2/15}$, $\eta_{3/24}$, $\eta_{4/28}$, or $\eta_{4/33}$ sheet composed of a DC framework with a twin-hexagonal hole at the center. This structure proves to be a sixth-order saddle point at B3LYP/6-311+G(d,p) and further optimization in the imaginary frequencies results in a three-dimension (3D) B_{26}. Interestingly, as expected, partial hydrogenation of D_{2h} B_{26} at each corner leads to the "glasses-shaped" D_{2h} $B_{26}H_8$ (**1a**) which maintains the planarity and high symmetry of the D_{2h} B_{26} core and is a true minimum on the potential energy surface of the system. $B_{26}H_8$ (**1a**) appears to have a large hydrogenation energy of −287.8 kcal/mol with respect to $B_{26} + 4H_2 = B_{26}H_8$. There exists a B–B bridge across the molecular center with the bond length of $r_{B-B} = 1.605$ Å. CMO analyses show that

this neutral molecule possesses 8 occupied delocalized π MOs with 16 electrons, while both its dication D_{2h} $B_{26}H_8^{2+}$ (**2a**) with a B–B bridge of $r_{B-B} = 1.707$ Å and the neutral C_{2h} $B_{26}H_6$ (**3a**) with a B–B bridge of $r_{B-B} = 1.702$ Å possess 7 occupied delocalized π MOs with 14 π electrons. The fact that **1a** possesses a shorter B–B bridge than both **2a** and **3a** shows that the 16 delocalized π electrons in **1a** makes the molecule somehow a bit more elongated than both **2a** and **3a** which have 14 delocalized π electrons. However, the $4n + 2$ Huckel rule can not be directly applied to such polycyclic hydroboron clusters to access their overall aromaticity, as discussed below in details.

Both the perfectly planar **1a** and **2a** are true minima of the systems, with **1a** lying 4.22 kcal/mol than the second lowest-lying 3D isomer (**1b**) and at least 30.33 kcal/mol lower than all the other low-lying isomers, and **2a** being 60.51 kcal/mol lower than the second lowest-lying triangular isomer (**2b**) and at least 70.93 kcal/mol lower than other cage-like or triangular motifs (see Fig. 1). Interestingly, the fourth isomer of $B_{26}H_8$ (**1d**) which contains a DC framework without the B–B bridge at the center appears to lie much higher in energy (36.2 kcal/mol) than **1a**, indicating that the B–B bridge plays a crucial role in maintaining the stability of the system. We notice that **3a** is a transition state with a small imaginary frequency at $23i$ cm^{-1}. Relaxing the structure in the imaginary frequency leads to slightly distorted C_2 $B_{26}H_6$ (**3a′**, see Fig. S4 in Supporting Information for the structure) which lies only 0.29 kcal/mol lower in energy. Such an energy differences is smaller than the ZPE difference of 0.4 kcal/mol between **3a** and **3a′**, so the perfectly planar C_{2h} $B_{26}H_6$ (**3a**) is expected to be the vibrationally averaged structure of $B_{26}H_6$. For simplicity, we choose to use the perfectly planar **3a** rather than non-planar **3a′** to discuss the properties of $B_{26}H_6$ in the following analyses.

Obviously, **1a**, **2a**, and **3a** share the same structural characteristics to contain a DC framework with a THH at the center which may serve as building blocks of stable MLBSs with THHs (see Fig. S1). Note that, due to the bond orientations and symmetry constrains, the B–B bonds in **1a**, **2a**, and **3a** have a much larger bond length fluctuation (between 1.58 and 1.83 Å) than that in $\eta_{4/33}$ and $\eta_{4/28}$ boron sheets (1.67–1.70 Å). However, the average B–B bond lengths in **1a**, **2a**, and **3a** are found to be about 1.67 Å, which is very close to corresponding value of 1.68 Å in $\eta_{4/33}$ and $\eta_{4/28}$ boron sheets [6, 12].

Although we can not guarantee that the bicyclic $B_{26}H_8$ (**1a**), $B_{26}H_8^{2+}$ (**2a**), and $B_{26}H_6$ (**3a**) are the global minima of these medium-sized binary clusters at current stage, the results obtained suggest that these twin-hexagonal hole structures are the most promising isomers in the experimental realization of these clusters, especially $B_{26}H_8^{2+}$ (**2a**) which seems to be a very deep minimum on the potential energy surface of the dication (similar to the previously reported perfect planar D_{6h} $B_{18}H_6^{2+}$ [26]). The calculated ionization potentials (IPs, at OVGF/6-311++G(d,p) level) and HOMO–LUMO energy gaps (ΔE_{gap}, at B3LYP/6-311++G(d,p) level) of $B_{26}H_8$ (**1a**) (7.54 and 1.17 eV) and $B_{26}H_6$ (**3a**) (6.22 and 1.51 eV) (see Table 1) support their high stabilities towards electron detachments. We notice that D_{2h} $B_{26}H_8^{2+}$ (**2a**) has an even wider HUMO–LUMO gap (1.86 eV). Such boron-rich clusters may be generated in gas phases where the thermodynamically favorable isomers have the superior priority to be detected.

Table 1 Calculated NICSzz/ppm and HOMO–LUMO energy gaps (ΔE_{gap}/eV) of D_{2h} $B_{26}H_8$, D_{2h} $B_{26}H_8^{2+}$ and C_{2h} $B_{26}H_6$, ionization potentials (IP/eV) of D_{2h} $B_{26}H_8$ and C_{2h} $B_{26}H_6$ at B3LYP/6-311+G(d,p), compared with D_{2h} $C_{16}H_{14}$ and D_{2h} $C_{10}H_8$ at the same theoretical level (calculated NICSzz values for the selected points in the molecular plane [NICSzz(0)] or 1.0 Å above the plane [NICSzz(1)])

	NICSzz(0)	NICSzz(1)	ΔE_{gap}	IP
D_{2h} $B_{26}H_8$				
a	47.6	23.1	1.17	6.28
b	−42.6	−23.3		
D_{2h} $B_{26}H_8^{2+}$				
a	−15.5	−33.3	1.86	–
b	−88.6	−60.6		
C_{2h} $B_{26}H_6$				
a	−12.0	−32.3	1.51	7.33
b	−87.9	−59.6		
D_{2h} $C_{16}H_{14}$				
a	62.6	47.2	1.72	6.91
b	−20.8	4.22		
D_{2h} $C_{16}H_{14}^{2+}$				
a	−29.2	−30.8	1.86	–
b	−90.0	−49.6		
D_{2h} $C_{10}H_8$				
a	−13.4	−29.1	4.75	7.97
b	−82.7	−42.6		

a: the center of one hole (0.0 Å and 1.0 Å above it)

b: the molecular center (0.0 Å and 1.0 Å above it)

Bonding Patterns and Aromaticities

Detailed AdNDP analyses present clear π and σ bonding patterns for these interesting molecules. As shown in Fig. 2, the eight π MOs of $B_{26}H_8$ (**1a**) can be classified into two groups, i.e. two six-center two-electron (6c-2e) π bonds in the central region across the B–B bridge and six five-center two-electron (5c-2e) π bonds along the DC framework around the twin-hexagonal hole with the occupation numbers |ON| = 1.90–1.91 |e|. Similarly, the seven delocalized π MOs of **2a** and **3a** also belong to two groups, one twelve-center two-electron (12c-2e) π bond in the central region across the B–B bridge and six 5c-2e π bonds along the DC framework with |ON| = 1.80–1.96|e|. Concerning the σ bonding interaction, AdNDP analyses show that both **1a** and **2a** have only one typical two-center two-electron (2c-2e) B–B σ bridge bond along the short C_2 molecular axis. Such a σ bridge is important to maintain the twin-hexgonal hole structure and without it, the bicyclic geometry will be converted to the very unstable isomer **1d** which contains an elongated decagonal hole. All the other twenty-six σ bonds in both **1a** and **2a** appear to be delocalized three-center-two-electron (3c-2e) bonds covering the whole DC framework. For **3a**, the 2c-2e B–B σ bridging bond and the twenty-two 3c-2e B–B σ bonds appear to be similar to that of **1a** and **2a**. The main difference occurs in the corner regions near

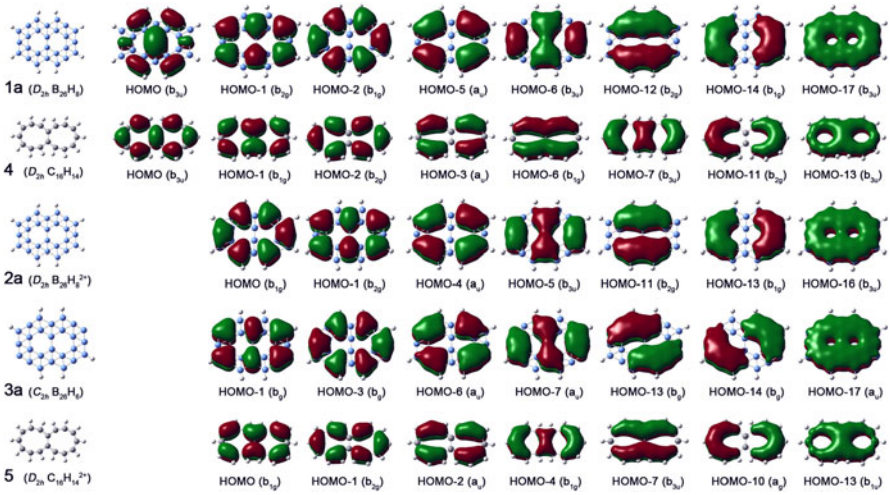

Fig. 2 Occupied π MOs of D_{2h} $B_{26}H_8$ (**1a**), D_{2h} $B_{26}H_8^{2+}$(**2a**), and C_{2h} $B_{26}H_6$(**3a**), compared with that of D_{2h} $C_{16}H_{14}$(**4**), and D_{2h} $C_{16}H_{14}^{2+}$(**5**)

the two vertex B atoms without –H terminals: the four 3c-2e B–B σ bonds and two 2c-2e B–H σ bonds in these regions in **1a** and **2a** are converted into four periphery 2c-2e σ bonds and two delocalized 4c-2e σ bonds over two B_4 rhombuses in **3a**.

Such delocalized bonds are expected to lead to the formation of islands of both π and σ aromaticity in these molecules, similar to the situations reported in the polycyclic aromatic hydroboron $B_{3n}H_m^{27}$ and DC planar B_nH_2 series[20]. These AdNDP bonding patterns are supported by both ELF and NICS analyses. It has been well established that aromatic molecules possess average bifurcation values [$ELF_{av} = (ELF_\sigma + ELF_\pi)/2$] greater than 0.70 in the interval of (0,1) [35]. As shown in Fig. 3, the ELFs of these molecules show the existence of delocalized π and σ interactions which are generally in line with the AdNDP bonding patterns discussed above. More importantly, both the ELF_π (0.85–0.88) and ELF_σ (0.76–0.78) bifurcation values and their average ELF_{av} (0.81–0.83) lie well above 0.70, indicating that these molecules are overall aromatic in nature in ELF criteria. $NICS_{zz}$ values which are site-dependent have been widely used as criteria of the aromaticity for planar molecules. As shown in Table 1 and Table S1, all the points studied at the center of the whole molecule, the centers of the two B_6 hexagon holes, and center of each B_3 triangle for $B_{26}H_8^{2+}$ (**2a**) and $B_{26}H_6$ (**3a**) possess negative $NICS(0)_{zz}$ and $NICS(1)_{zz}$ values, indicating that they are overall aromatic with the formation of island aromaticity. Similarly, $B_{26}H_8$ (**1a**) possesses negative $NICS(0)_{zz}$ and $NICS(1)_{zz}$ values at the center of the whole molecule and at the center of each B_3 triangle. However, these negative $NICS_{zz}$ values appear to be systematically smaller than the corresponding values of $B_{26}H_8^{2+}$ (**2a**) and $B_{26}H_6$ (**3a**) and more importantly, $B_{26}H_8$ (**1a**) has positive $NICS_{zz}$ values at centers of the two B_6 hexagon holes (see Table 1). We conclude that these bicyclic molecules are all overall aromatic in nature with the formation of both π and σ island aromaticity, though $B_{26}H_8$ (**1a**) with 16 delocalized π electrons ($4n$, $n = 4$) possesses somehow a

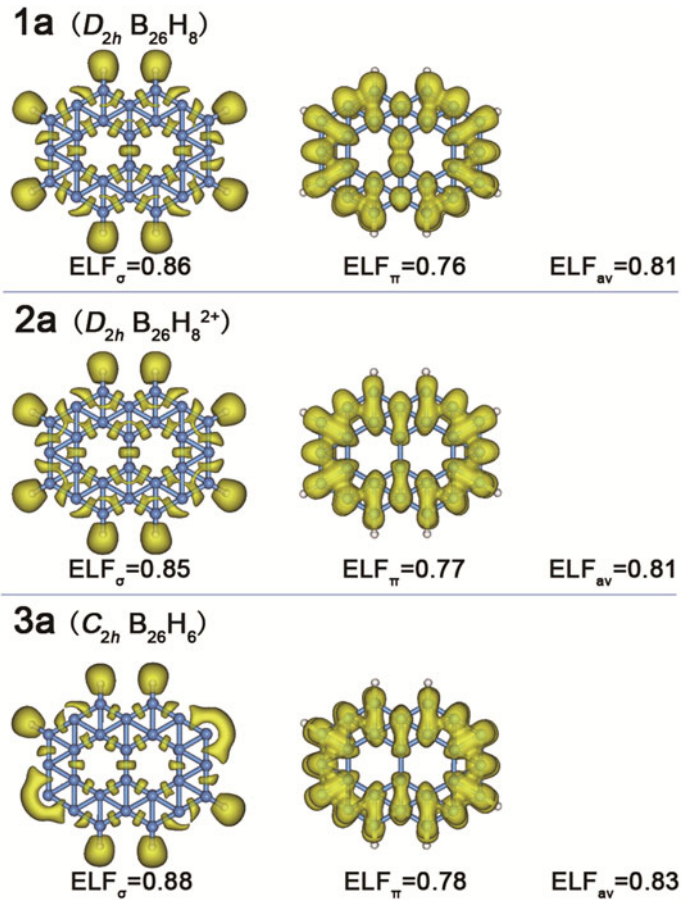

Fig. 3 σ- and π-ELFs of **1a**, **2a**, and **3a** with the estimated ELF_σ and ELF_π bifurcation values and their average values (ELF_{av}) indicated

weaker aromaticity than $B_{26}H_8^{2+}$ (**2a**) and $B_{26}H_6$ (**3a**) which both have 14 delocalized π electrons and formally satisfy the Huckel rule ($4n + 2$, $n = 3$). Interestingly, as shown in Table 1, the calculated $NICS_{zz}$ of $B_{26}H_8^{2+}$ (**2a**) and $B_{26}H_6$ (**3a**) appear to be comparable with the corresponding $NICS_{zz}$ values of aromatic $C_{16}H_{14}^{2+}$ and $C_{10}H_8$.

Comparison with Hydrocarbons

We continue to compare these aromatic hydroboron clusters with their bicyclic hydrocarbon counterparts which look similar in molecular shapes. Geometrically, the former possess a DC framework while the latter possess a single-chain (SC) framework. Boron DCs in these hydroboron clusters are equivalent to the carbon SCs in the corresponding hydrocarbons (except the B–B bridge across the DC

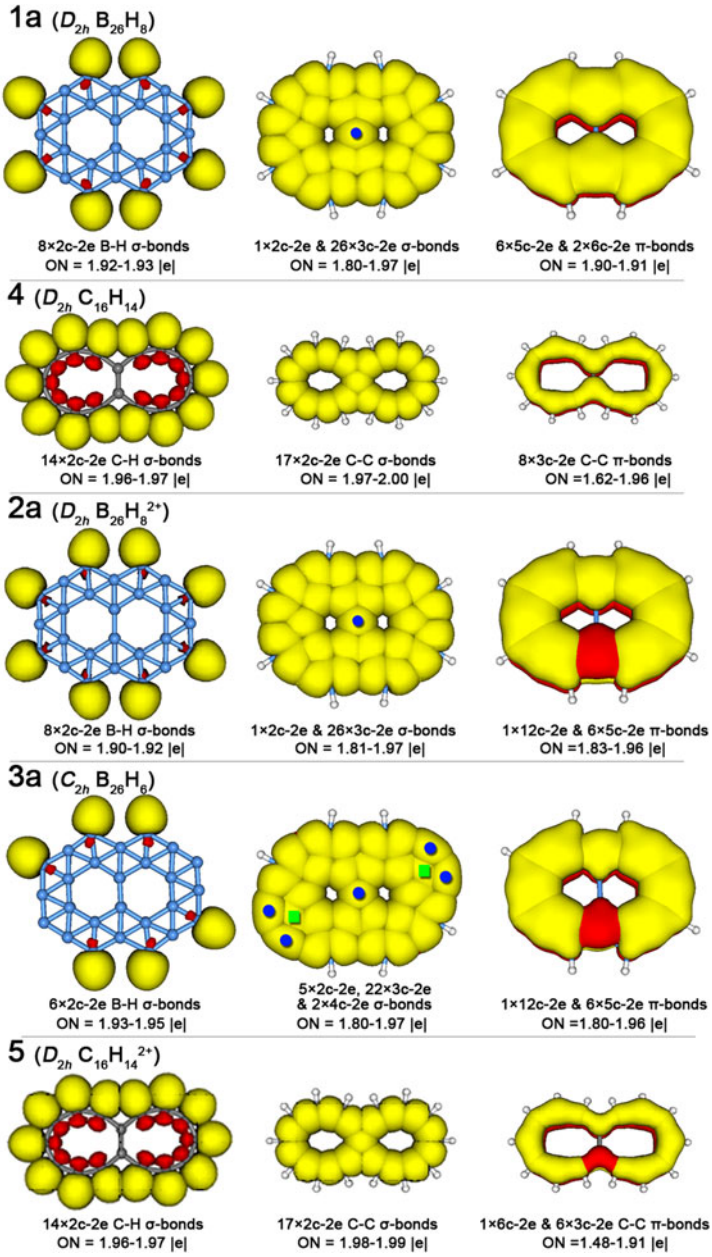

Fig. 4 AdNDP analyses of **1a**, **2a**, **3a**, and their bicyclic hydrocarbon counterparts **4** and **5**. "ON" denotes the occupation number, blue cycle dots denote the 2c-2e B–B σ bonds, and green rectangles denote the 4c-2e B–B σ bonds. Note that the 12c-2e B–B-bonds of **2a** and **3a** are delocalized in the central regions across the B–B bridge

framework in the former). Such an interesting geometrical relationship also exists in the previously reported $B_{18}H_6^{2+}$ [26] and $B_{30}H_8$ [27]. Electronically, as shown in Fig. 2, the occupied delocalized π MOs of $B_{26}H_8$ (**1a**) have the one-to-one correspondence relationship with that of bicyclic D_{2h} $C_{16}H_{14}$ (**4**), simultaneously, $B_{26}H_8^{2+}$ (**2a**), and $B_{26}H_6$ (**3a**) have the similar relationship (though the energy order may be different) with that of the bicyclic D_{2h} $C_{16}H_{14}^{2+}$ (**5**) (note that **4** and **5** are hypothetic molecules as high-order stationary points on their potential energy surfaces), respectively. As demonstrated in Fig. 4, the AdNDP π bonding patterns of **1a**, **2a**, and **3a** with delocalized bonding characteristics also appear to be similar with that of their bicyclic hydrocarbon counterparts which contain mainly localized π bonds (2c-2e π bonds). The main difference between them occurs in their σ bonding patterns. **1a**, **2a**, and **3a** possess mainly delocalized 3c-2e or 4c-2e σ bonds along the DC framework around the twin-hexagonal hole (except the B–B bridge), while their hydrocarbon counterparts have only localized 2c-2e σ bonds.

Such a π plus σ double delocalization can be traced back to the electron deficiency nature of boron. Natural bond orbital (NBO) analyses show that average total natural bond orders of boron atoms in these clusters lie between 3.98 and 4.23, indicating that the identified delocalized bonds along the DC framework can effectively compensate the electron deficiency of boron and satisfy its bonding requirements. Obviously, DCs are the narrowest "boron belts" to form π plus σ double delocalization. We address here that all stable MLBSs predicted to date are overwhelmingly dominated by either extended or zigzag DCs [7–14] and the perfectly planar hydroboron clusters D_{6h} $B_{18}H_6^{2+}$ [26] and D_{2h} $B_{30}H_8$ [27] presented previously and D_{2h} $B_{26}H_8$ predicted in this work may sever as the building blocks of these boron sheets, as demonstrated in Fig. S1 and the Table S1.

Summary

We have performed in this work an extensive DFT investigation on planar D_{2h} $B_{26}H_8$ (**1a**), D_{2h} $B_{26}H_8^{2+}$(**2a**), and C_{2h} $B_{26}H_6$(**3a**) which possess a DC framework and may serve as the building blocks of stable boron sheets with THHs. Detailed CMO, NICS, ELF, and AdNDP analyses indicate that they are overall aromatic in nature and analogous to D_{2h} $C_{16}H_{14}$ (**4**), and D_{2h} $C_{16}H_{14}^{2+}$ (**5**) in π bonding, respectively. As the energetically the lowest-lying isomers obtained, these bicyclic hydroboron clusters form interesting molecules to model the nucleation and growth processes of MLBSs. Future experimental syntheses and characterizations of these bicyclic hydroboron clusters through laser ablation of boron targets in H_2-seeded gaseous phases may enrich the chemistry of boron hydrides and establish an interesting analogy relationship between hydroborons and hydrocarbons.

Acknowledgments This work was jointly supported financially by the NSFC (No. 20873117, 21003086, and 21273140) and SXNSF (No. 2010011012-3). The authors thank Dr. Qiang Chen for helpful discussion.

References

1. A. R. Oganov, J. Chen, C. Gatti, Y. Ma, Y. Ma, C. W. Glass, Z. Liu, T. Yu, O. O. Kurakevych, and V. L. Solozhenko (2009). *Nature* **457**, 863.
2. I. Boustani, in Chemical Modelling: Applications and Theory, by Springborg M., (RSC Publishing, London, 2011), pp. 1-44.
3. J. Kortus, K. D. Mazin II, V. P. Belashchenko, Antropov, and L. L. Boyer (2001). *Phys. Rev. Lett.* **86**, 4656.
4. D. Ciuparu, R. F. Klie, Y. M. Zhu, and L. Pfefferle (2004). *J. Phys. Chem. B* **108**, 3967.
5. F. Liu, C. Shen, Z. Su, X. Ding, S. Deng, J. Chen, N. Xu, and H. Gao (2010). *J. Mater. Chem.* **20**, 2197.
6. I. Boustani, A. Quandt, E. Hernandez, and A. Rubio (1999). *J. Chem. Phys.* **110**, 3176.
7. H. Tang and S. Ismail-Beigi (2007). *Phys. Rev. Lett.* **99**, 115501.
8. I. Boustani, A. Rubio, and J. A. Alonso (1999). *Chem. Phys. Lett.* **311**, 21.
9. E. S. Penev, S. Bhowmick, A. Sadrzadeh, and B. I. Yakobson (2012). *Nano Lett.* **12**, 2441.
10. X. Wu, J. Dai, Y. Zhao, Z. Zhuo, J. Yang, and X. C. Zeng (2012). *ACS Nano* **6**, 7443.
11. X. Yu, L. Li, X.-W. Xu, and C.-C. Tang (2012). *J. Phys. Chem. C* **116**, 20075.
12. H. G. Lu, Y. W. Mu, H. Bai, Q. Chen, and S. D. Li (2013). *J. Chem. Phys.* **138**, 024701.
13. A. N. Alexandrova, A. I. Boldyrev, H.-J. Zhai, and L.-S. Wang (2006). *Coord. Chem. Rev.* **250**, 2811.
14. H. J. Zhai, B. Kiran, J. Li, and L. S. Wang (2003). *Nat. Mater.* **2**, 827.
15. B. Kiran, S. Bulusu, H. J. Zhai, S. Yoo, X. C. Zeng, and L. S. Wang (2005). *Proc. Natl. Acad. Sci. USA* **102**, 961.
16. A. P. Sergeeva, D. Y. Zubarev, H.-J. Zhai, A. I. Boldyrev, and L.-S. Wang (2008). *J. Am. Chem. Soc.* **130**, 7244.
17. W. Huang, A. P. Sergeeva, H.-J. Zhai, B. B. Averkiev, L.-S. Wang, and A. I. Boldyrev (2010). *Nat. Chem.* **2**, 202.
18. A. P. Sergeeva, B. B. Averkiev, H.-J. Zhai, A. I. Boldyrev, and L.-S. Wang (2011). *J. Chem. Phys.* **134**, 224304.
19. A. P. Sergeeva, Z. A. Piazza, C. Romanescu, W. L. Li, A. I. Boldyrev, and L. S. Wang (2012). *J. Am. Chem. Soc.* **134**, 18065.
20. D. Z. Li, Q. Chen, Y. B. Wu, H. G. Lu, and S. D. Li (2012). *Phys. Chem. Chem. Phys.* **14**, 14769.
21. H. L. Yu, R. L. Sang, and Y. Y. Wu (2009). *J. Phys. Chem. A* **113**, 3382.
22. N. G. Szwacki, V. Weber, and C. J. Tymczak (2009). *Nanoscale Res. Lett.* **4**, 1085.
23. H. Bai and S.-D. Li (2011). *J. Clust. Sci.* **22**, 525.
24. Q. Chen and S. D. Li (2011). *J. Clust. Sci.* **22**, 513.
25. W. L. Li, C. Romanescu, T. Jian, and L. S. Wang (2012). *J. Am. Chem. Soc.* **134**, 13228.
26. Q. Chen, H. Bai, J. C. Guo, C. Q. Miao, and S. D. Li (2011). *Phys. Chem. Chem. Phys.* **13**, 20620.
27. H. Bai, Q. Chen, Y. F. Zhao, Y. B. Wu, H. G. Lu, J. Li, and S. D. Li (2013). *J. Mol. Model.* **19**, 1195.
28. A. D. Becke (1993). *J. Chem. Phys.* **98**, 5648.
29. C. Lee, W. Yang, and R. G. Parr (1988). *Phys. Rev. B* **37**, 785.
30. P. P. Bera, K. W. Sattelmeyer, M. Saunders, H. F. Schaefer, and P. V. Schleyer (2006). *J. Phys. Chem. A* **110**, 4287.
31. B. B. Averkiev, Geometry and electronic structure of doped dluster via the Coalescence Kick method. Ph.D. Dissertation (2009) Utah State University, Logan, Utah.
32. D. Y. Zubarev and A. I. Boldyrev (2008). *Phys. Chem. Chem. Phys.* **10**, 5207.
33. D. Y. Zubarev and A. I. Boldyrev (2008). *J. Org. Chem.* **73**, 9251.
34. D. Y. Zubarev and A. I. Boldyrev (2009). *J. Phys. Chem. A* **113**, 866.
35. J. C. Santos, J. Andres, A. Aizman, and P. Fuentealba (2005). *J. Chem. Theory Comput.* **1**, 83.
36. P. v. R. Schleyer, C. Maerker, A. Dransfeld, H. Jiao, and N. J. R. v. E. Hommes (1996). *J. Am. Chem. Soc.* **118**, 6317.
37. P. v. R. Schleyer, H. Jiao, N. J. R. v. E. Hommes, V. G. Malkin, and O. Malkina (1997). *J. Am. Chem. Soc.* **119**, 12669.
38. Z. F. Chen, C. S. Wannere, C. Corminboeuf, R. Puchta, and P. v. R. Schleyer (2005). *Chem. Rev.* **105**, 3842.
39. K. Wolinski, J. F. Hinton, and P. Pulay (1990). *J. Am. Chem. Soc.* **112**, 8251.
40. M. J. Frisch, et al. in Gaussian 03 Revision A.01, Gaussian Inc. (2004) Wallingford.